ICAS 2021 SHANG HAI
International Council of the Aeronautical Sciences
32nd Congress of the International Council of the Aeronautical Sciences
September 6-10, 2021
Pudong Shangri-La, Shanghai, China

VIRTUAL PROTOTYPING OF ELECTRICAL THSA FOCUSED ON MECHANICAL POWER TRANSMISSION FUNCTIONS

Jian FU[1], Chaoqun ZHENG[1], Jean-Charles MARE[2] & Wensen ZHANG[1]

[1]School of Mechanical Engineering and Automation, Beihang University, Beijing 100191, China
[2]Institute Clément Ader (CNRS UMR 5312), INSA-Toulouse, Toulouse 31077, France

Abstract

Trimmable horizontal stabilizer actuator (THSA) system is a safety-critical system for flight controls. It is not accepted that the THS steering is free to vary under airload which would cause a total loss of control of aircraft pitch in case of actuation fail to fault. The preferred ultimate response to a THSA fault consists in freezing its position by designing a so-called fail-freeze actuator. This is achieved by combining specific mechanical functions in the power paths and loads. However, very little literature has introduced these functions and addressed the modelling and simulation activities from a system-level point of view. This paper addresses the system-level virtual prototyping of an electrical THSA, which is also a type of redundant electromechanical actuator (EMA) for more electric aircraft. Emphasis is put on the modelling and simulation of mechanical functions that are involved to get a fail-freeze design. The models are developed with resort to the Bond Graph formalism, considering their technical realization with both power and signal views. A particular attention is paid to the models' architectures, interfaces and causalities to facilitate the reuse, integration and implementation of the models, in any relevant simulation platform.

Keywords: Bond-Graph, EMA, Dual Path, Modeling and Simulation, More Electric Aircraft

1. Introduction

As the development of electric technologies in aerospace industry, both economic and environmental issues are improved. [1] More electric power technological advancements are used in the latest aircrafts and is towards to "more electric" and even "all electric" concepts. [2,3] In this situation, some primary and key secondary fight controls have applied novel "power-by-wire" technology to replace conventional "power-by-pipe" designs. [4,5] This is beneficial for reducing aircraft weight and fuel consumption. Therefore, the two types of electrically powered actuators, Electro-Hydrostatic Actuator (EHA) and Electro Mechanical Actuator (EMA) are greatly developed and come in the front of actuation service. EHAs remove the central hydraulic power networks and integrate a local one. They have been implemented e.g. in the Airbus A350 as backup and Lockheed Martin F-35 as active mode for aileron, rudder and elevators. EMAs eliminate all the hydraulic circuits. They are used in civil aircraft like Boeing B-787 for secondary flight controls of spoilers, braking and trimmable horizontal stabilizer (THS) only.[6] The maturity level of EMAs is behind that of EHAs for primary flight controls, because EMAs lack of viable solutions to avoid jamming in the limit of weight and installation space.[7,8] However, the electromechanical technology has the advantages of safer operations and easier maintenance. [9] It can be considered as the ultimate actuation technology for "all electric aircraft".

At present stage, an electrical THSA has attracted more and more attention. It is considered as a special EMA by introducing redundant paths and mechanical power management devices to implement the fault-tolerant function for applying in a safety-critical flight control. It can achieve collection of failure data. [10,11] The Trim Horizontal Stabilizer (THS) of an aircraft is the horizontal surface of the tail wing, which is cooperating with the elevator for controlling pitch. Generally, the movement of the THS is fine adjusted by the THSA in order balance the moments around the aircraft pitch axis,

without resort to any steering of the elevators. [12] The conventional THSA is hydraulically powered. It is driven by two hydraulic motors, such as in A320/A330/B777. Then with the development of more electric technology, THSA became firstly hybrid powered by two hydraulic motors and one electric motor, e.g. on the Airbus A-380. [13] Nowadays, compared to the conventional THSA, the original hydraulic power source is removed and replaced by the electric one, done on Airbus A350/B787 and COMAC C919. Whatever the way used to supply the THSAs, the key technology deals with the mechanical power transmission design, which integrates the redundant load paths and ensure a safe response to a failure. Johnsen proposed a novel concept with two primary load paths [12], and Wachendorf [14] presented a $H\infty$ mixed sensitivity controller design approach with two primary load paths on the basis of a conventional hydraulic THSA. In the present communication, the electrical THSA under study involves two electric motors to drive a redundant gearbox that transmits the mechanical power to the THS surface.

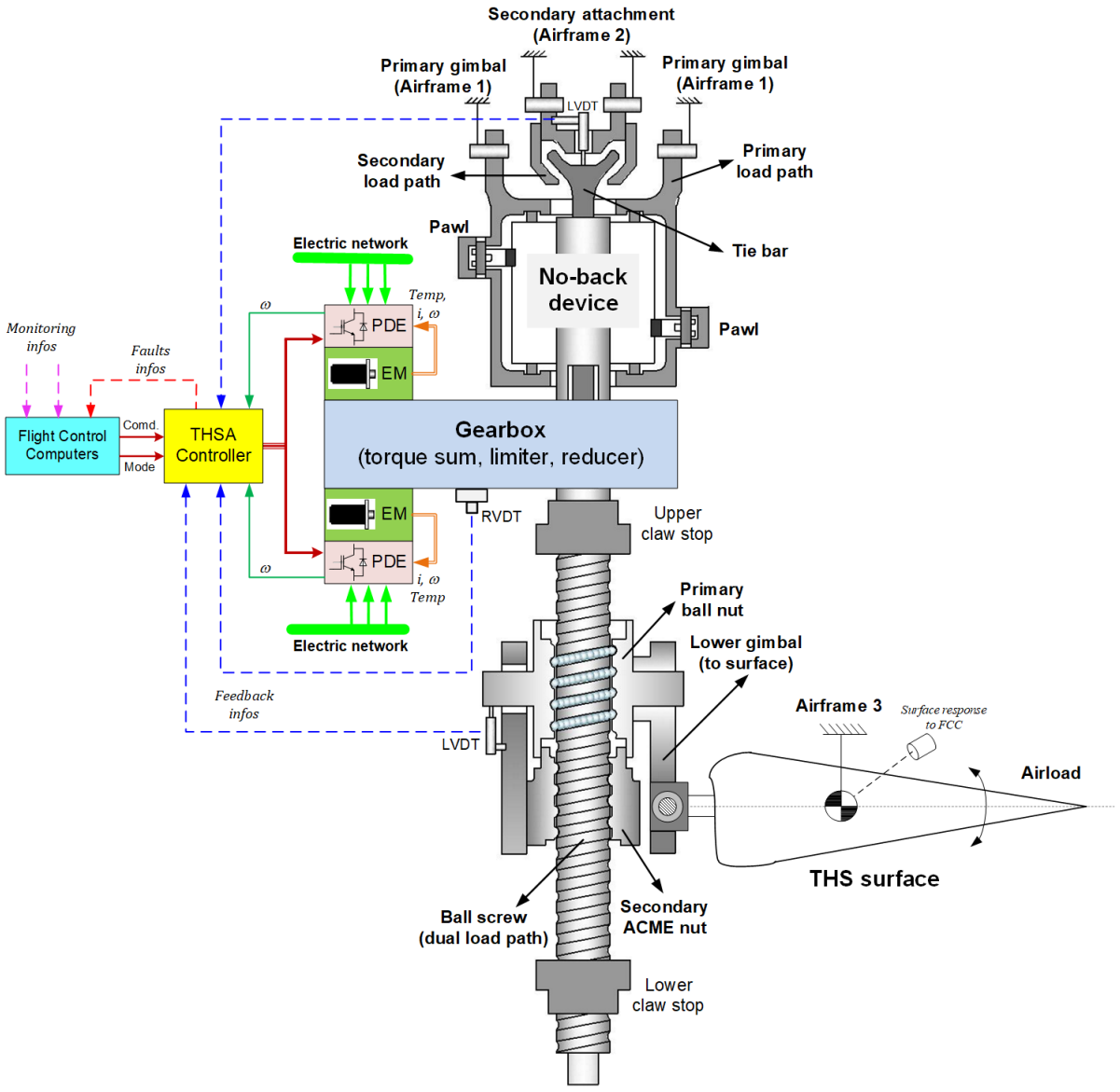

Figure 1 – Example of electrical THSA system.

To ease the diffusion of EMAs for future first flight controls and landing gear applications, advanced redundant structure and failure to safe mode of mechanical power transmission of THSA is of particular interest for further research. However, there is very little literature addressing the operation of the THSA mechanical power transmission, supported by system-level modeling and simulation including both multidisciplinary effects and failure to safe performance of faults. For this reason, the focus is put in this paper on the modeling and simulation of the mechanical power transmission and management

functions of an electrically-supplied THSA. Section 2 descripts the considered THSA. Then primary and secondary load paths are presented in detail. In section 3, multidisciplinary models are designed based with support of the Bond-Graph formalism. Section 4 analyzes the safe critical mechanical faults. Section 5 presents the results of simulations and enables the function performed to be verified through a model-based approach.

2. Electrical THSA System Description

This paper deals with an electrical THSA, which architecture is shown in Figure.1. Two high-speed electric motors are used to convert electric power into the mechanical power. They are combined in an active-standby dual function and integrate each an independent brake. A gearbox has the main features of torque summing, torque limiter and reducer for transmitting the motors power to the screw-shaft of a ball-screw mechanism. Two concentric load paths are used to ensure structural redundancy, including an active-standby dual screw-nut design. In that manner the THSA realizes a redundant motorized bar of the 3-bar kinematics linking the THS and the airframe. The control structure considered for such a THSA system is implemented in open position loop, and only the velocity is controlled.

2.1 Major Components and Functions

In this paper, it is considered that the electrical THSA system consists of the following components:

- Electronics: the THSA controller performs only the velocity control loop, the positions are monitored only. The Power Drive Electronics (PDE) control the amount of power flowing between the electrical networks and the electric motors.
- Electric motors: two Permanent Magnet Synchronous Machines (PMSMs) are equipped with an individual Power-Off Brake (POB).
- Gearbox: a torque-summed one transmits rotational mechanical power to the screw-shaft assembly.
- Ball screw-nut: a dual redundant screw-nut is made on an active ball-nut and a passive ACME nut, the passive nut being not loaded in normal mode.
- Upper and lower attachments: the upper primary gimbal attachment and the No-Back device belong to the primary load path. The upper secondary lug attachment and tie rod belong to the secondary load path. The Lower gimbal assembly connects the dual nuts to the THS surface.
- Mechanical stops: upper and lower claw stops provide the backup mean to limit the ball screw retract and extend run-away movement in case the software limits fail.
- Sensors: motor current, velocity and temperature sensors provide signal for control and monitoring. Two Rotational Variable Differential Transducers (RVDTs) are used to measure the screw-shaft angular velocity. Two position sensors of Linear Variable Differential Transformers (LVDTs) type are used for integrity checks, one on the upper gimbal assembly and the other on the lower gimbal mechanism. They are used to detect a failure of the primary load path and a failure of the primary ball nut, respectively.
- THS Surface: the linear motion of the nuts is transformed into rotary motion of the THS using a 3-bar kinematics.

2.2 Primary and Secondary Load Path

In order to meet the safety requirements, usually, dual redundancy load path of mechanical power transmission is implemented in THSA. The primary load path is active in normal operation. It consists in a rotating ball screw, a No-Back device, an upper primary gimbal assembly connected to the airframe and a translating primary ball nut driving the THS surface. Oppositely, the secondary load path is normally unloaded thanks proper backlash with the primary one. It consists of a tie rod located inside the ball screw, an upper secondary lug attached to the aircraft fuselage, and a secondary nut.

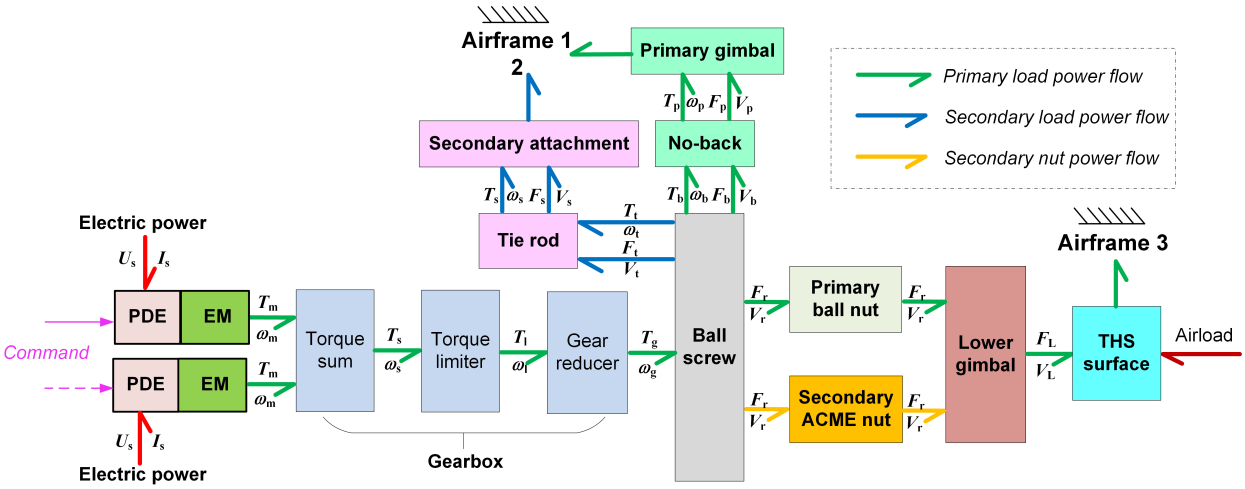

Figure 2 – Functional power flow of electrical THSA.

In the event of any component of primary load path failed (wear or rupture), the backlash is eliminated, and the secondary load path becomes loaded. However, the secondary load path is designed to subject to a smaller airload because it is specified to operate for a very short-time till to landing safely: the failure is detected by flight control computers, and then THS surface is be locked by combination of different means to get fail-freeze actuation response. The electrical THSA is decomposed into modules using the Bond-Graph formalism according to its physical structure. The functional power flow is shown in Figure 2. Typically, power flows from the electric supply network through the PDE from electric network is converted into rotational mechanical power by the motors and the gearbox assembly, is then converted to translational mechanical power by the nut-screw, and finally to rotary mechanical power through the 3-bar kinematics to actuate the THS surface.

3. Multidisciplinary Models Design

Electrical THSA has the numerous multi-domains, cross-linked physical effects found in EMAs: electric, magnetic, mechanical and thermal. In order to follow the system engineering process, the model-based system-level virtual prototyping is facilitated by the use of the Bond-Graph formalism. The models are developed considering their technical realization with a power view instead of a pure signal view. A particular attention is paid to the models' architectures, interfaces and causalities to facilitate the reuse, adaption, integration and implementation of the models in any other relevant simulation environment. By this way, the development time and risk are be reduced is the models are properly validated for use in a virtual prototyping approach. Thus, it is here proposed to decompose the THSA into the main package models according to the functional power flow path in Figure 2.

3.1 PDE

The PDEs modulate the power flowing between the electrical network and the electric motor by acting on the motor winding voltages. From the functional point of view, the PDE can be seen as a modulated power transformer. However, this transformation does not come without power losses coming from switching and conduction of transistors and diodes.

The principle and model of PDE and electric motor have been previously studied in details, e.g. in [15]. This communication focuses on the functional architectures and interfaces the power level mainly. So, the modelling and control of the PDE is not addressed in details below.

3.2 Electric Motor and Gearbox

The PMSM motors convert electric energy into mechanical energy. The POB are contributed to hold the THS angular position when the No-Back mechanism fails or other similar faults occur. A velocity closed-loop control is implemented with a PID controlled. The THSA velocity demand is set to null when the THSA nut reaches the desired position.

The gearbox of the THSA can be functionally divided into torque summing, torque limitation and gear reduction. The mechanical compliance of the different elements of the gearbox is considered globally, introducing the overall stiffness (k_g) and equivalent viscous damping (d_g). The inertia of the gearbox is also considered as a single equivalent inertial element (J_g).

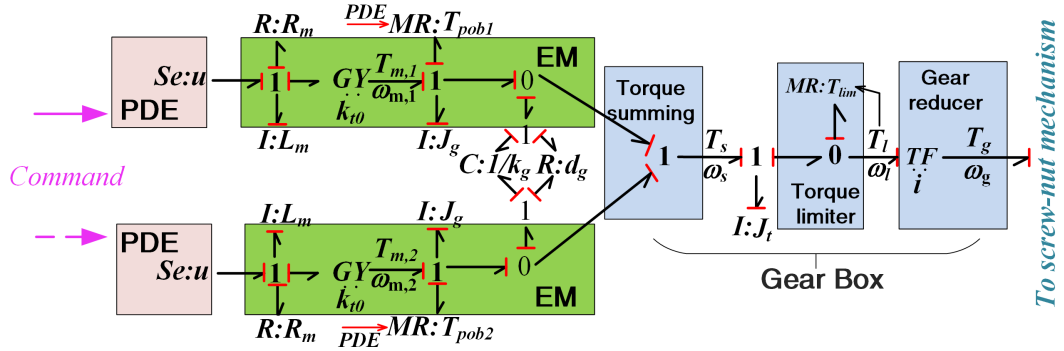

Figure 3 – Bond Graph model of gearbox.

The torque (T_m) transmitted from the dual motors firstly passes through the POB which is modelled at a high level by a modulated resistive element (MR) mounted in series (1 junction) in the power flow, as shown in Figure 3. The Boolean modulation signal of the brake is issued by the PDE. Then the torque is summed in the gearbox using the 1 junction. The torque limiter is used to protect the motor from additional phase current while the airload exceeds expectations. This function is realized by friction discs. It is again modelled at a system level as a modulated resistive element (MR) but mounted in parallel (0 junction). This time, the friction torque of the torque limiter is a non-linear function of the output torque (T_l).
Through the gear reducer, the torque is increased to fulfill the load demand with a low weight and volume motor. It is composed of multi-stage gears. The multi-stage gear reducer is viewed at a system level as an equivalent perfect power transformer (TF) of ratio i. The output of gearbox can be derived:

$$\begin{cases} T_g = i\,(T_{m,1} + T_{m,2}) \\ \omega_{m,1} + \omega_{m,2} = i\omega_g \end{cases} \tag{1}$$

Where T_m and T_g represent the output torque of the dual motors and the torque transformed from gearbox respectively while ω represents the rotation speed.

3.3 Mechanical Power Transmission

The screw-nut mechanism is a significant component in the model of THSA. It converts the rotational velocity and torque from the gearbox into the linear speed and force to drive the trimmable horizontal stabilizer surface. The functional model of THSA considers a series of three effects from the gearbox to the surface: equivalent inertia at screw-shaft level, perfect screw-nut and equivalent compliance effect at screw-nut. The global inertia of the THS is modelled as an inertance element I of parameter J_{bs}. The while the perfect screw-nut model achieves a power transformation of ratio $(2\pi/p)$ as follows:

$$\begin{cases} F_r = T_g 2\pi/p \\ v_r = \omega_g p/2\pi \end{cases} \tag{2}$$

Where p is the lead of the screw. For simplification, the compliance effects are considered as a pure compliance element C of stiffness (k_b) with a parallel dissipative element R of damping parameter d_b. While v_r is the speed of the screw, the contact elastic force (F_e) and the damping force (F_d) are considered as follows:

$$\begin{cases} F_e = k_b \int v_r dt \\ F_d = d_b v_r \end{cases} \tag{3}$$

In order to meet the safety requirements, the redundancy load path of mechanical power transmission (MPT) is implemented. The ACME nut will be loaded when the primary load path of ball nut failed. The perfect transmission and compliance effects are considered in the redundancy load path. As shown in Figure 4, the dotted line represents unloaded. The force and torque are also transported to the No-Back mechanism (F_b T_b) and tie-rod (F_t T_t).

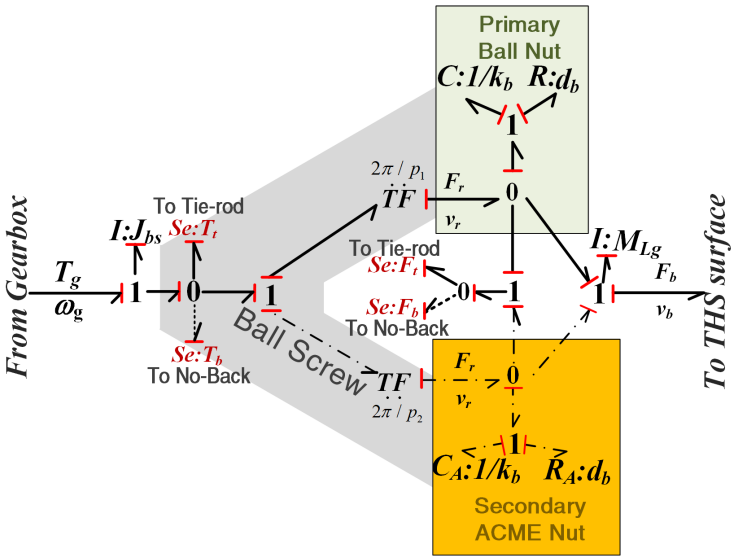

Figure 4 – Bond Graph model of MPT.

3.4 No-Back Mechanism

The No-Back mechanism is installed to make the THS irreversible in case loss of both actuation channels. The function of the No-Back mechanism is thus to prevent the airload from driving the surface backward. A detailed drawing of a friction No-Back is provided in [13]. The No-Back is mainly composed of two ratchet-pawl assemblies and two friction discs. The pawls are used to limit avoid any motion of the ratchet wheel when the THS operates as an aiding load.

As shown in Figure 5, the No-Back mechanism includes No-Back assembly and primary gimbal which connects to the airframe. It is reduced as a pair of ratchet-pawl assembly and friction disc for the convenience of modeling. The force (F_b) transmitted from the MPT is applied to the friction disc to produce friction torque which simplified to a modulation source element. Inertia (J_{nb}) and mass (M_{nb}) are considered respectively in torque transmission path and force transmission path. The compliances of No-Back mechanism and primary gimbal are simplified as the contact stiffness(k_{pg}) and damping(d_{pg}), which represented as a pair of resistive element and capacitive element. Besides, the capacitive element of No-Back mechanism is modulated for the backlash between the ratchet wheel and pawl.

3.5 Tie Rod Mechanism

The tie-rod mechanism is part of the secondary load path which is normally unloaded thanks to the reserved proper backlash. As shown in Figure 6, the backlash is represented as a capacitive element C in the secondary attachment. When the primary load path fails, the secondary load path becomes loaded while the tie-rod mainly bears the force to avoid the free movement of the THS surface. In that case, the mass of the tie-rod (M_{tb}) should be considered for causality reasons in simulation. The compliances of tie-rod mechanism are simplified as a global capacitance effect of stiffness (k_{tb}) and damping (d_{tb}). The model of secondary attachment is similar in structure to the primary gimbal. It connects the fuselage and the tie-rod.

3.6 THS Surfacem

The force (F_b) and velocity (v_b) from the gearbox are transmitted to the THS surface through the lower gimbal, and the airload on the surface is expressed by a modulation effort source element SE. For

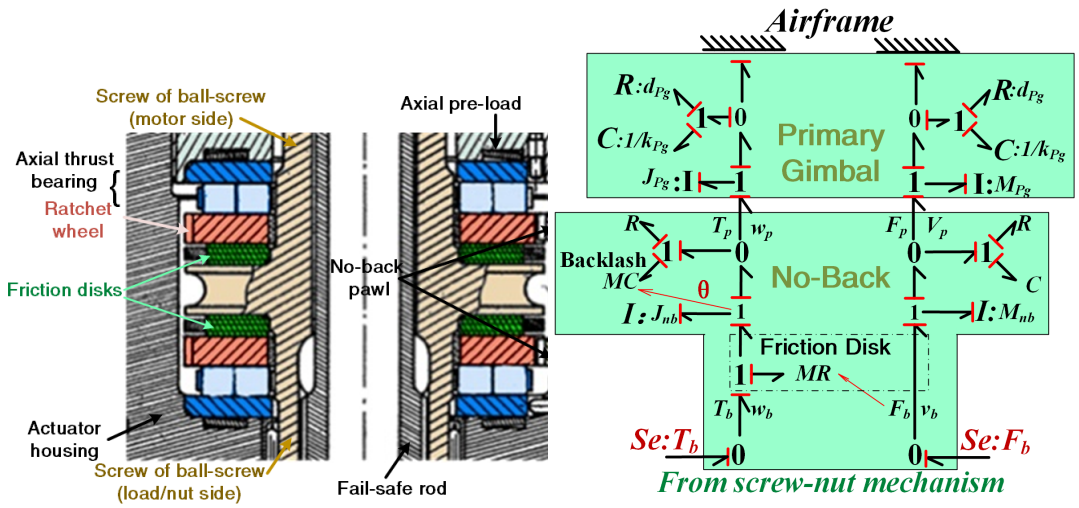

Figure 5 – No-back with friction disks(left: sectional view of no-back[13]; right: Bond Graph model of No-Back mechanism)

simplification, the compliance effects of lower gimbal are considered as a spring damper element for the stiffness (k_g) and the damping (d_g). The contact elastic force (F_{e2}) and the damping force (F_{d2}) are considered as follows:

$$\begin{cases} F_{e2} = k_g \int v_b dt \\ F_{d2} = d_g v_b \end{cases} \tag{4}$$

As shown in Figure 7, the mass of the surface (M_{THS}) and the lower gimbal (M_{Lg}) should also be considered to meet causality constraints. Assuming that the airload acts on the far end of the surface. Considering the installation points of THS pivot to airframe and upper/lower attachments to airframe/THS surface, a ratio k is needed to present the geometric relation between the force of airload acting on the fuselage and to the nut screw load path.

4. Safe Critical Mechanical Faults

Considering safety requirements, the failures related to such a critical THSA system must be taken into account to avoid any hazardous and catastrophic event by the inability to hold the position of the THS with respect to the airframe. From the point of view of power and signal, the root causes leading to such a THSA failure can be classified into electrically, magnetically, thermally and mechanically ones. The electrical and magnetic faults come from the control electronics, PDE, motors, brakes and sensors. They are extensively documented in the scientific literature. The thermal faults in aerospace actuators are difficult to address through system level simulation and require a 3-D distributed- parameters modelling. The complex redundant load and power path in a THSA comes from the risk freeing the THS position. Thus, the simulation of faults and the analysis of corresponding THSA responses potentially provide rich means to address reliability and health monitoring. The mechanical faults can be generically introduced in the model follows to address.

4.1 Mechanical Power Transmission

As a probably result of the mechanical wear, excessive loading and structural fatigue, the faults occurred in the breakage connection between two mechanical elements:

- Mechanical drive: motor and gearbox, gearbox reducer and ball screw;
- Load path: ball screw shaft and No-Back/upper gimbal assembly, ball nut and lower gimbal assembly, tie rod and upper secondary lug, ACME nut and lower gimbal assembly.

In order to model the loss of load transmission, they can be modeled by modulated the mechanical stiffness and damping effects of the connection between bodies. Although modulating a C effect in a Bond-Graph does not ensure energy conservation, it is accepted here because long term energy conservation in the model is not mandatory.

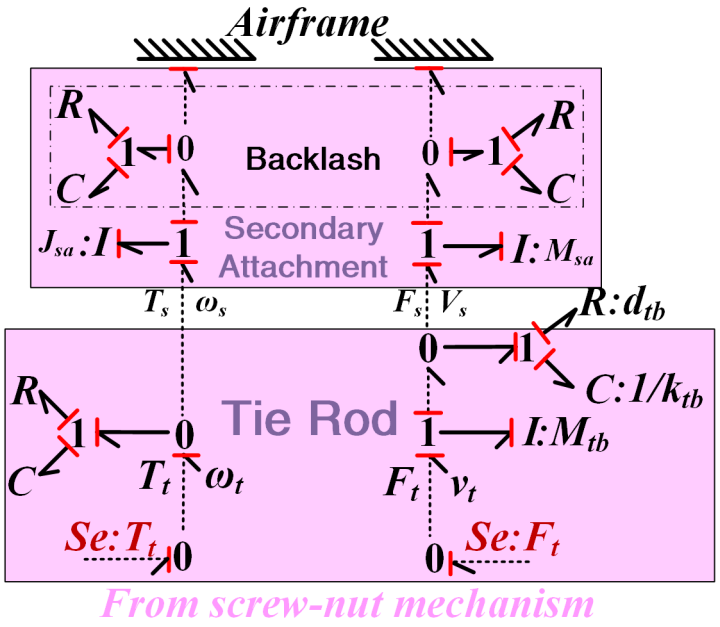

Figure 6 – Bond Graph model of tie-rod mechanism.

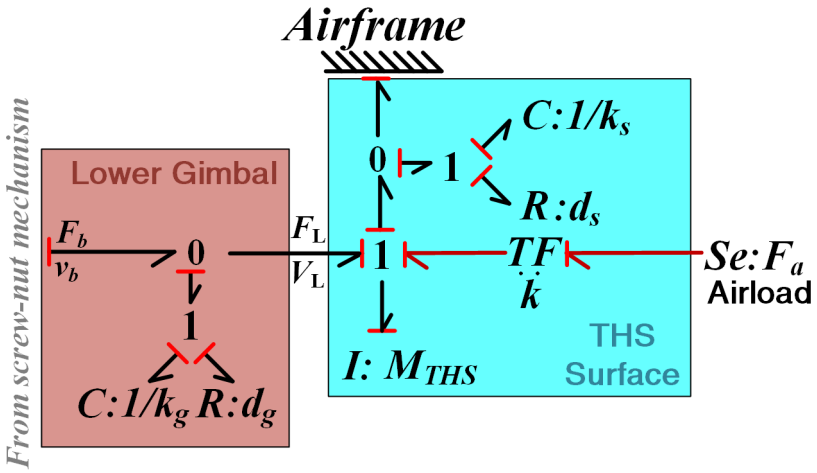

Figure 7 – Bond Graph model of THS surface.

4.2 Internal Mechanical Components

The bearings, planetary gears, screw balls and friction disks are the main subcomponents in THSA mechanical components. Rupture, fracture or increased backlash can be introduced like in section 4.1 by alteration of the backlash, stiffness and damping parameters. If interesting, jamming can be modelled increasing friction.

4.3 External Surface Attachments

THSA system has four attachments: upper primary gimbal assembly connects to airframe, upper secondary lug connects to airframe, lower gimbal assembly to THS surface and THS pivoting joint to airframe. The failures are always from the structure fatigue or the excessive airload effort, these also can be introduced by breakage and jam effects as mentioned earlier.

5. Validation of Models

The electrical THSA model has been introduced in section 3. The virtual prototype of the electrical THSA implemented in the multidomain system-level simulation environment, Siemens-AMESim, with special attention to the mechanical domain and less interest to control. Emphasis is put on

the modelling and simulation of mechanical functions that are combined to get a fail-freeze design. The implementation and reuse of the Bond-Graph model are facilitated through the extensive use of standard models available in the software libraries.

5.1 Control Strategy

As already mentioned, the control strategy of the studied THSA is based on velocity feedback. In Figure 8, the PDE is considered as a perfect modulated power transformer. Based on this model, the influence energy losses and thermal effect are ignored. The electromagnetic torque produced by the motor acts directly on the motor shaft inertia. The speed of the shaft is used as the feedback to form a velocity closed-loop control, with an addition the torque limitation by control. In the follow-up study of the electric THSA model, an active/active motor control is adopted. The control strategy remains simplified and does not intend to equalize torque between motoring channels.

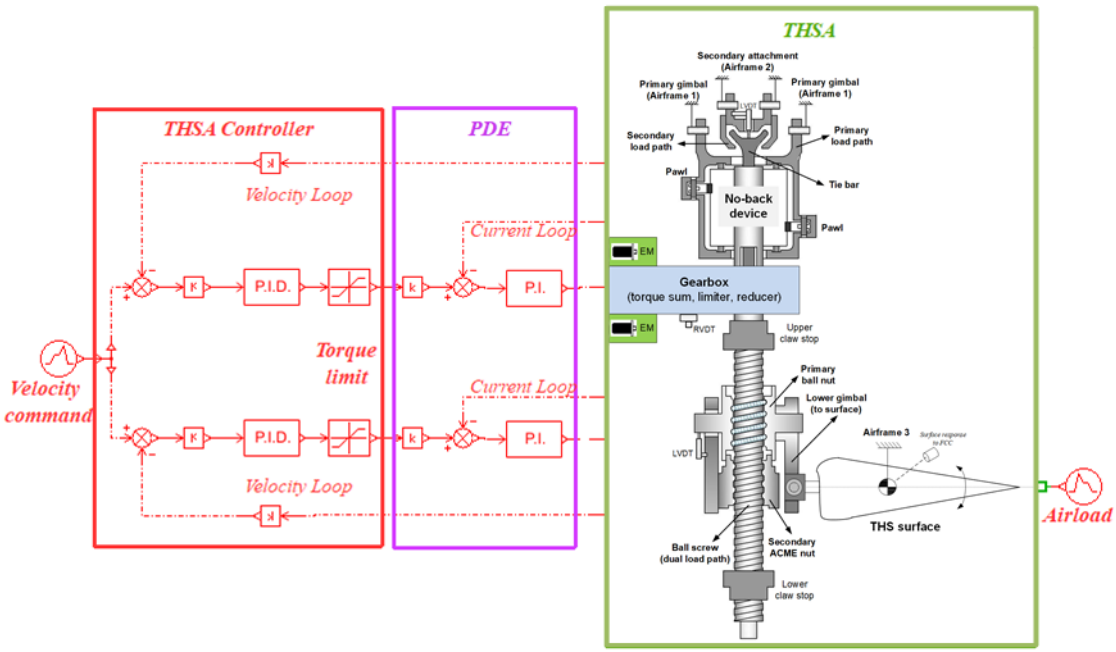

Figure 8 – Basic control model for electrical THSA.

5.2 Implementation of the Model

The controller and the ideal PDE model described above are packaged as super components, and the overall electrical THSA model is shown in Figure 9. The layout position of each component assembly corresponds to the physical architecture shown in section 2. The model is implemented in the Siemens-AMESim simulation platform, according to the structure provided by the Bond-Graph given in section 3.

There are some points that need extra attention: the torque limiter involves a friction model between two rotating bodies and the level of friction is calculated as a function of the output torque. The No-Back is modelled using the same generic friction model but the level of friction is computed as a function of the axial force from THS to screw and the angular velocity of the screw. In that manner, it is possible to make the friction level dependent on the power quadrant of operation of the THSA (aiding or opposite load). The compliance effect is based on the generic sub-model of a spring/damper. Super components are made to enable stiffness, damping and backlash to be varied dynamically. In the ball screw mechanism, the primary ball nut and secondary ACME nut also use super components, which can also inject faults and enable the effective load sharing between redundant paths to be observed. The sub model mass with displacement limit is selected for the lower gimbal mass, and the limit of actuator extension distance is calculated according to the surface deflection angle. The simulation parameters of the model are summarized in Table 1.

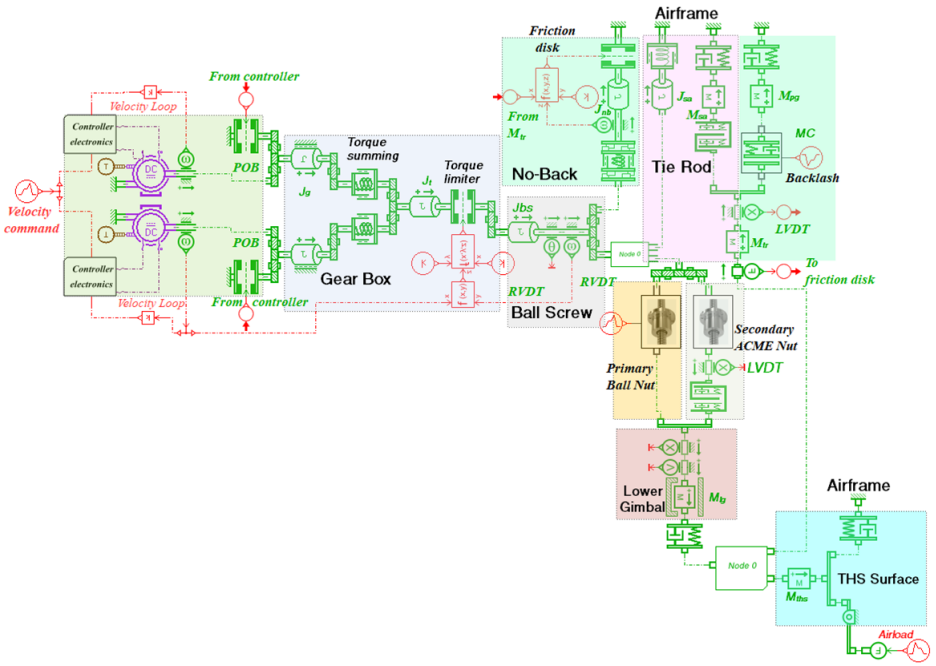

Figure 9 – Functional model of electrical THSA in AMESim.

Table 1 – Simulation parameters of the electrical THSA.

Parameter	Symbol	Value	Unit
Motor shaft inertia	J_g	1.4e-4	kgm^2
Motor winding resistance	R_m	0.89	Ω
Motor winding inductance	L_m	1.95	mH
Torque constant	k_{t0}	0.2	$V/(rad/s)$
Maximum Coulomb friction torque of POB	T_{POB}	2.5	Nm
Inertia of gear	J_t	9.02e05	kgm^2
Maximum Coulomb friction torque of torque limiter	T_{lim}	10	N_m
Overall gear ratio	i	70.5	-
Inertia of screw nut mechanism	J_{bs}	0.105	kgm^2
Lead of screw	p	12.7	mm
Contact stiffness of ball screw mechanism	k_b	2e+08	N/m
Contact damping of ball screw mechanism	d_b	1e+04	$N/(m/s)$
Mass of lower gimbal	m_{lg}	22	k_g
Tare torque of the No-Back mechanism	T_{nb}	10	Nm
Inertia of No-Back mechanism and primary gimbal	$J_{nb}+J_{pg}$	3e-03	kgm^2
Mass of No-Back mechanism and primary gimbal	$m_{nb}+m_{pg}$	25	Kg
Contact stiffness of No-Back mechanism	k_{nb}	5e+08	N/m
Contact damping of No-Back mechanism	d_{nb}	1e+06	$N/(m/s)$
Inertia of tie rod	J_{tr}	3e-03	kgm^2
Mass of tie rod	m_{tr}	20	kg
Contact stiffness of tie rod mechanism	k_{tr}	2e+08	N/m
Contact damping of tie rod mechanism	d_{tr}	1e+05	$N/(m/s)$
Contact stiffness between THSA and surface	k_g	5e+08	N/m
Contact damping between THSA and surface	d_g	1e+06	$N/(m/s)$
Equivalent mass of surface	m_{ths}	100	kg
Connection stiffness between rudder and fuselage	k_s	2e+05	N/m
Connection damping between rudder and fuselage	d_s	1e+04	$N/(m/s)$

5.3 Simulation Verification

The rapidity, stability and accuracy of the model are tested by the step speed response and ramp speed response. By injecting the signal into the super component, the fault of the electric THSA is simulated, so as to verify the correct response of the redundant design and the fail-freeze function.

5.3.1 Step Response

In order to verify the step response of the system, a speed command is set as a 15mm/s step occurring at t=0.5s. When the speed is stable, at t=1s, an equivalent 30kN airload step is applied to observe the load rejection capability of the speed control. It can be seen from Figure 10 that the speed step response of the THS actuation system is fast: given the model parameters, the rise time is less than 0.1s, there is basically no overshoot and steady-state error. At t=2s, the given speed command is set again to zero. Due to the inertia and the clearance of ratchet and the pawl, the phenomenon of reverse drive appears. However, when the clearance is eliminated, there is no more reverse driving phenomenon. At t=3s, due to the impact caused by the clearance elimination of ratchet and pawl, the speed response is delayed. It can be seen from the right figure that the change of ratchet pawl clearance and the surface deflection angle in the whole moving process.

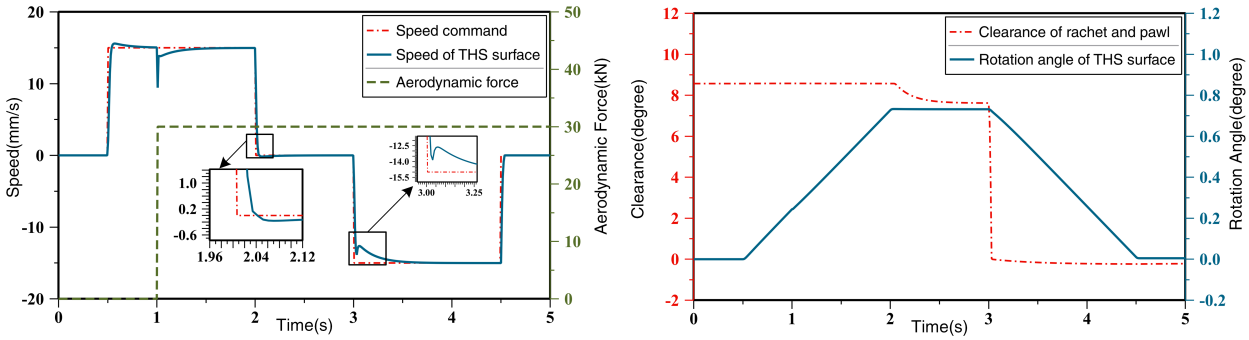

Figure 10 – Step Response of the healthy electrical THSA.

5.3.2 Ramp Response

As shown in Figure 11, the airload is set to increase from 0kN to 30kN after 1s, and the speed command is increased from 0 to 15mm/s with a 15mm/s2 acceleration. It can be seen that the speed tracking performance is good. It also appears negative acceleration due to the clearance between rachet and pawl, but eliminated quickly.

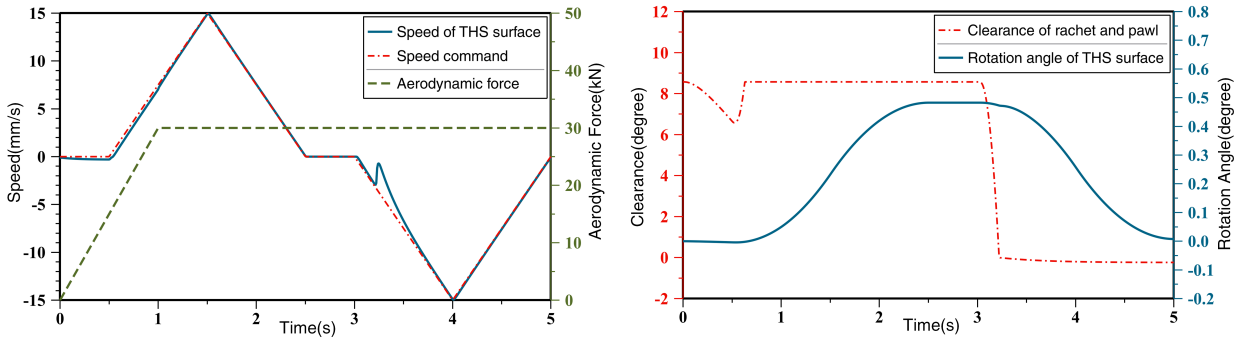

Figure 11 – Ramp response of the healthy electrical THSA.

5.3.3 Response to Primary Load Path Fault

By increasing the clearance between the upper gimbal and the fuselage, the failure of the primary load path is simulated. The simulation results are shown in the Figure 12. The clearance of the super element of the upper gimbal is increased at 2.5s, the clearance of the secondary load path is eliminated, the force of the safety tie rod increases, and the load is transmitted through the secondary

load path. As shown in Figure 12, the speed feedback fluctuated due to the switching of load paths at 2.5s.

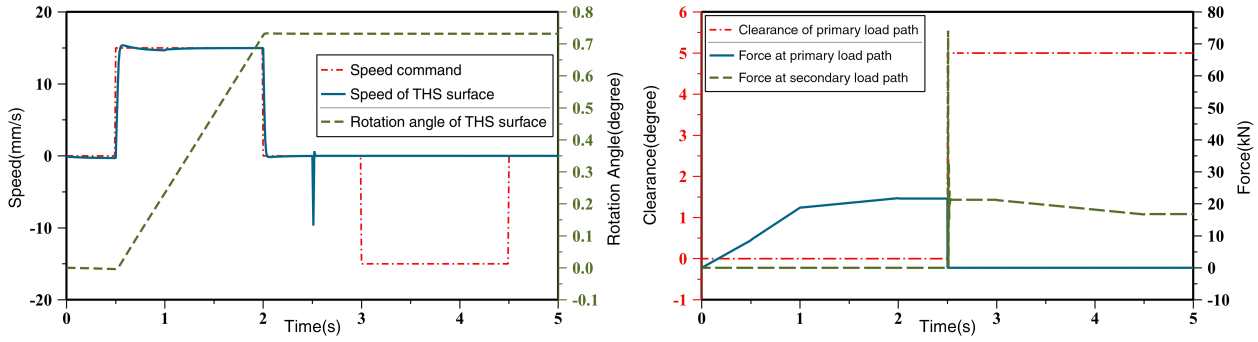

Figure 12 – Response to primary load path fault.

5.3.4 Response to Primary Ball Nut Fault

When the speed mode is changed from low speed 9mm/s to high speed 15mm/s, the clearance of primary ball nut is increased to simulate the failure of primary load path and the switch of the secondary ACME nut screw pair. As shown in Figure 13, when the injection fault occurs at t=3s, the clearance of the primary ball nut super component is increased which indicated the primary ball nut fails. The clearance of the secondary ACME nut is eliminated, and all the force becomes hold by the secondary nut. It can be seen from the figure that the clearance value of the secondary ACME nut is cancelled when it becomes active.

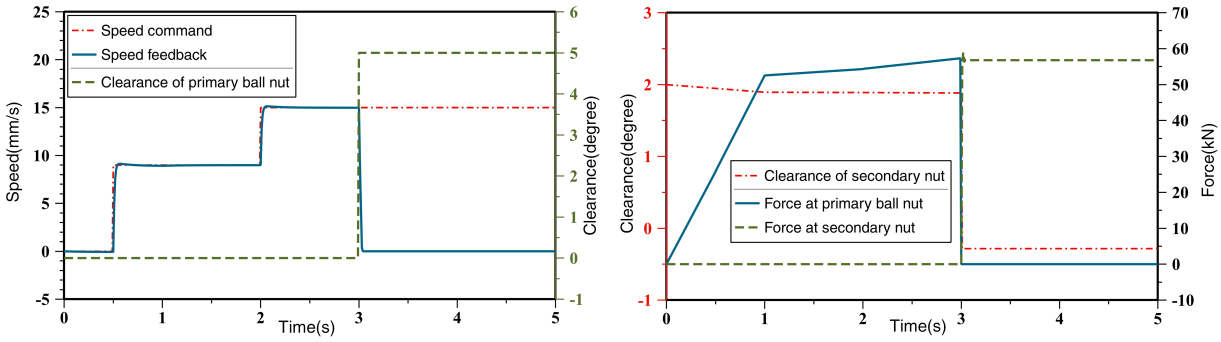

Figure 13 – Response to primary ball nut fault.

5.3.5 Verification of No-Back Mechanism

In order to verify the correct behavior of the No-Back mechanism, the airload is progressively increased until the torque produced the motor cannot offset the airload. In this condition the load tends to back drive the THSA. The clearance between the ratchet and the pawl of the No-Back mechanism is eliminated. The pawl blocks the ratchet motion and the airload is counteracted by the friction torque generated between the rotating friction disk and the blocked racket. The THS surface is locked, and the actuator is in fail-freeze mode. As shown in Figure 14, when the airload is increased to 100kN at t=3.5s, the clearance between ratchet and pawl is eliminated. The steering of the THS surface remains constant.

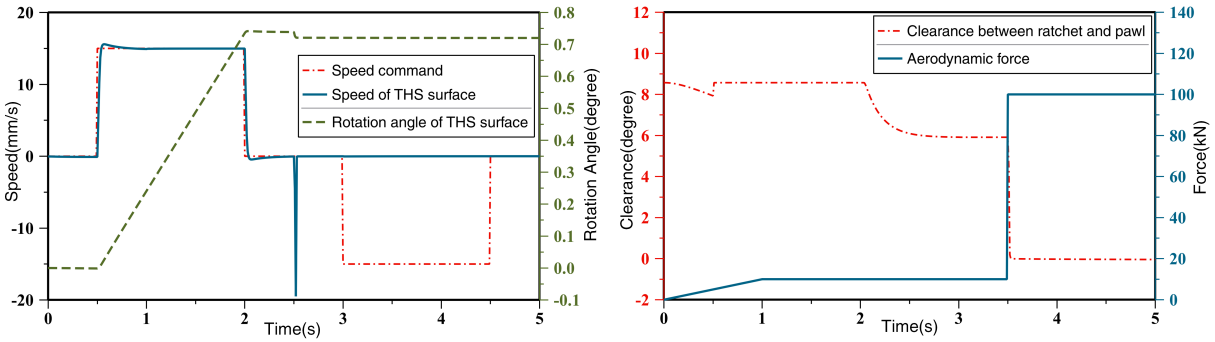

Figure 14 – Verification of No-Back mechanism.

6. Conclusion

This paper has addressed the system-level virtual prototyping of an electrical THSA. An exemplary architecture has been introduced considering the major functions to be performed and the components involved for their embodiment. The Bond-Graph formalism has been extensively used for architecting the THSA model and facilitating its implementation in a commercial simulation software. The main mechanical faults leading a loss of a power or load pass have modelled and the response to these faults have been simulated and analyzed. The virtual prototyping of the electrical THSA has been used to verify the correct response of the redundant design in the presence of a mechanical fault. As expected from the requirement, the mechanical redundancies provide the THSA with a fail-freeze capability, which is confirmed by simulation of a the detailed. The performance of the model and the freezing mode are verified by simulation of the proposed model.

7. Contact Author Email Address

The contact author email address is, Dr. Jian FU: fujian@buaa.edu.cn

8. Copyright Statement

References

[1] Lafage R, Aubry S and Junior A. The Clean Sky Technology Evaluator: review and results of the environmental impact assessment at mission level. 16th AIAA Aviation Technology, Integration, and Operations Conference, Washington DC USA, AIAA 2016-3745, pp 1-10, 2016.

[2] Roboam X, Sareni B and Andrade A D. More electricity in the air: Toward optimized electrical networks embedded in more-electrical aircraft. IEEE Industrial Electronics Magazine, Vol. 6, No. 4, pp 6-17, 2012.

[3] Bulent S and Casey T M. More Electric Aircraft: Review, Challenges, and Opportunities for Commercial Transport Aircraft. IEEE Transactions on Transportation Electrification, Vol. 1, No. 1, pp 54-64, 2015.

[4] Maré J-C. Aerospace Actuators 2: Signal-by-Wire and Power-by-Wire. 1st edition, ISTE & WILEY, 2017.

[5] Maré J-C and Fu J. Review on signal-by-wire and power-by-wire actuation for more electric aircraft. Chinese Journal of Aeronautics, Vol.30, No.3, pp 857-870, 2017.

[6] Fu J, Maré J-C and Fu Y. Modelling and simulation of flight control electromechanical actuators with special focus on model architecting, multidisciplinary effects and power flows. Chinese Journal of Aeronautics, Vol.30, No.1, pp 47-65, 2017.

[7] Todeschi M and Baxerres L. Airbus-Health Monitoring for the Flight Control EMAs. Proceeding of Recent Advances in Aerospace Actuation Systems and Components, Toulouse France, pp 73-83, 2014.

[8] Mazzoleni M, Previdi F, Scandella M and Pispola G. Experimental Development of a Health Monitoring Method for Electro-Mechanical Actuators of Flight Control Primary Surfaces in More Electric Aircrafts. IEEE Access. Vol.7, pp 153618-153634, 2019.

[9] Pier C B, Matteo D. L, Paolo M and Guido R. Design and Development of a Planetary Gearbox for Electromechanical Actuator Test Bench through Additive Manufacturing. Actuators, Vol.9, No. 35, pp 1-12, 2020.

[10] Arriola D and Thielecke F. Design of fault-tolerant control functions for a primary flight control system with electromechanical actuators. Proceedings of IEEE International Automatic Testing Conference, National Harbor USA, pp 478-482.

[11] SAE Aerospace. Trimmable Horizontal Stabilizer Actuator Descriptions. SAE AIR6052, pp 1-38, 2011.

[12] Johnsen S and Thielecke F. Integration analysis of trimmable horizontal stabilizer actuators and technology evaluation. CEAS Aeronautical Journal, Vol. 2011, No. 2, pp 11-19, 2011.

[13] Maré J-C. Aerospace Actuators 3: European Commercial Aircraft and Tiltrotor Aircraft. 1st edition, ISTE & WILEY, 2018.

[14] Wachendorf N, Thielecke F, Carl U and Pe T. Multivariable controller design for a trimmable horizontal stabilizer actuator with two primary load paths. 26th International Congress of the Aeronautical Sciences, Alaska USA, pp 1-12, 2008.

[15] Fu J, Maré J-C, Yu L and Fu Y. Multi-level virtual prototyping of electromechanical actuation system for more electric aircraft. Chinese Journal of Aeronautics, Vol.31, No.5, pp 892-913, 2018.